



HAL
open science

Two-dimensional continua capable of large elastic extension in two independent directions: asymptotic homogenization, numerical simulations and experimental evidence

E. Barchiesi, F Dell’Isola, François Hild, Pierre Seppecher

► To cite this version:

E. Barchiesi, F Dell’Isola, François Hild, Pierre Seppecher. Two-dimensional continua capable of large elastic extension in two independent directions: asymptotic homogenization, numerical simulations and experimental evidence. *Mechanics Research Communications*, 2020, 103, pp.103466. 10.1016/j.mechrescom.2019.103466 . hal-02404383

HAL Id: hal-02404383

<https://hal.science/hal-02404383v1>

Submitted on 11 Dec 2019

HAL is a multi-disciplinary open access archive for the deposit and dissemination of scientific research documents, whether they are published or not. The documents may come from teaching and research institutions in France or abroad, or from public or private research centers.

L’archive ouverte pluridisciplinaire **HAL**, est destinée au dépôt et à la diffusion de documents scientifiques de niveau recherche, publiés ou non, émanant des établissements d’enseignement et de recherche français ou étrangers, des laboratoires publics ou privés.

Two-dimensional continua capable of large elastic extension in two independent directions: asymptotic homogenization, numerical simulations and experimental evidence

E. Barchiesi, F. dell’Isola, F. Hild and P. Seppecher

Abstract

The synthesis of a 1D full second gradient continuum was obtained by the design of so-called *pantographic beam* (see Alibert et al. *Mathematics and Mechanics of Solids* (2003) [2]) and the problem of the synthesis of planar second gradient continua has been faced in several subsequent papers: in dell’Isola et al. *Zeitschrift für angewandte Mathematik und Physik* (2015) [5] and dell’Isola et al. *Proceedings of the Royal Society A: Mathematical, Physical and Engineering Sciences* (2016). [4] it is considered a three-length-scale microstructure in which two initially orthogonal families of long Euler beams (i.e. beams much longer than the size of the homogenization cell but much slenderer than it) are interconnected by perfect or elastic pivots (hinges). The corresponding homogenized two-dimensional continuum (which was called *pantographic sheet*) has a D4 orthotropic symmetry. It has been proven to have a deformation energy depending on the second gradient of in-plane displacements and to allow for large elongations in some specific directions while remaining in the elastic regime. However, in pantographic sheets, the deformation energy only depends on the geodesic bending of the actual configuration of its symmetry directions (see for more details Steigmann et al. *Acta Mechanica Sinica* (2015) [3] and Placidi et al. *Journal of Engineering Mathematics* (2017) [6]). On the other hand, in Seppecher et al. *J. of Physics: Conference Series* vol. 319 (2011) [1], it was designed a *bi-pantographic architected sheet* where the previously considered Euler beams were replaced by pantographic beams to form a more complex three-length-scale microstructure and it was proven that, once homogenized, such a bi-pantographic sheet, in planar and linearized deformation states, produces a more complete second gradient two-dimensional continuum. Derivatives of elongations along the two symmetry directions now appear in the deformation energy. The aim of the present paper is the experimental validation of the second gradient behavior of such bi-pantographic sheets. As their intrinsic mechanical structure produces a geometrically non-linear behavior for relatively small total deformation, we first need to extend the homogenization result to the regime of large deformations. Subsequently

we compare the predictions obtained using such second gradient model with experimental evidence, as elaborated by local Digital Image Correlation (DIC) focused on the discrete kinematics of the hinges.

1 Introduction

In physical literature the problem of synthesis has been confronted in many contexts. Namely, given a Lagrangian potential (describing the conservative part of considered phenomena) and a Rayleigh dissipation potential, specified in terms of suitable kinematic descriptors, one has to find a physical system, belonging to a class specified *a priori*, whose evolution is governed by the corresponding Hamilton-Rayleigh principle.

In the period (1930-1970) in which the prevalence of digital computers was not yet achieved, the problem of synthesis of electric circuits was confronted in order to design suitable, and dedicated, analog computers (see, e.g., Kron [13, 14]). When the *a priori* class of physical systems is constituted by electric circuits with only passive elements, the previous general problem was particularized as follows: given quadratic Lagrangian and Rayleigh potentials, in terms of a finite number of degrees of freedom, one has to find the graph of a circuit and the interconnecting (linear and passive) electric elements such that it is governed by the corresponding Hamilton-Rayleigh principle.

The available results found in the literature for the synthesis of passive electric circuits were recently used to synthesize *piezoelectromechanical metamaterials*, suitably tailored to dampen out mechanical vibrations (see dell’Isola et al. [15, 16, 17] and [18, 25]).

The synthesis problem for mechanical metamaterials reads as: given any choice of the continuous fields describing a kinematics, given functionals expressing the deformation energy, the kinetic energy and the dissipation potential in terms of these fields, find the architected mechanical structure (possibly multi-scale) such that, in the homogenization limit, the obtained continuous model is exactly the one chosen *a priori*. Therefore, the qualitative behaviour of a metamaterial shall be given by its multi-scale architecture rather than by the constituting base materials [31].

After the 2000s, in addition to the study on the synthesis of first gradient continua [23, 24], the synthesis of second gradient continua has been discussed and solved in the linear and conservative case for 1D, 2D and 3D continua (see [2, 4, 1, 5] and [7, 8]). In [9] and then in [10] a synthesis of couple-stress 3D and 2D continua has been obtained. Couple-stress continua (see [11]) are a particular case of second gradient continua. If F denotes the placement gradient, and its polar decomposition $F = RU$ is introduced, couple-stress continua are those whose deformation energy only depends on ∇R .

In [2] the problem of synthesizing a beam whose deformation energy (in the case of planar and linearized strains) depends on the second gradient of both axial and transverse components of displacement was solved by introducing so-called *pantographic beams* (see Fig. 1). The homogenization of pantographic beams in non-linear strain regime has been subsequently addressed in [20, 21].



Figure 1: Schematics of pantographic beam.

In [5, 4] an architected three-length-scale *pantographic sheet* was designed. It was a first solution to the problem of the determination of a microstructure whose homogenization produces a second gradient 2D continuum that is not a couple-stress continuum. The basic idea [4] was to consider an architected microstructure formed by two families of Euler beams, initially orthogonal (generalization have been developed in this respect [26]), which are interconnected by perfect or elastic pivots (hinges) (see Fig. 2). This architected microstructure has a D_4 orthotropic symmetry, whose material symmetry directions are those of the beams.

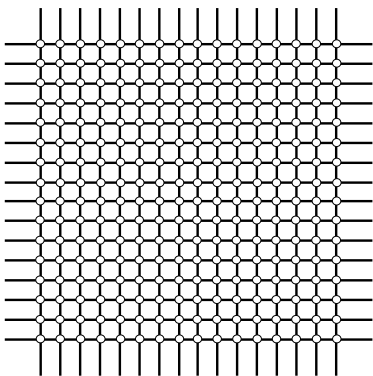


Figure 2: Schematics of pantographic sheet.

The concept underlying such a synthesis process is clear: when the structure is subjected to a global deformation, the beams are bent and therefore the macroscopic deformation energy must account for this phenomenon, and thus depends on geodesic curvature of

the current configuration of the material symmetry directions (i.e. on the second derivatives of material lines' transverse displacements along corresponding material symmetry directions for linearized strains, see also [22]). A global deformation is possible without bending any of the beams (see Fig. 3). However, its homogenized deformation energy does not depend on the full gradient of in-plane displacements and the capacity of large deformation is only restricted to a single specific deformation mode.

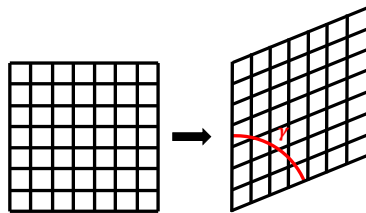


Figure 3: Zero-energy deformation mode for pantographic sheet.

To find a more complete second gradient 2D continuum [1], a bi-pantographic sheet, i.e. a D_4 symmetric material synthesized for getting a deformation energy depending on the derivatives along the symmetry directions of the corresponding elongations, has been proposed. The basic idea exploited there consists in replacing the long Euler beams constituting pantographic sheets with previously mentioned pantographic beams (see Fig. 4).

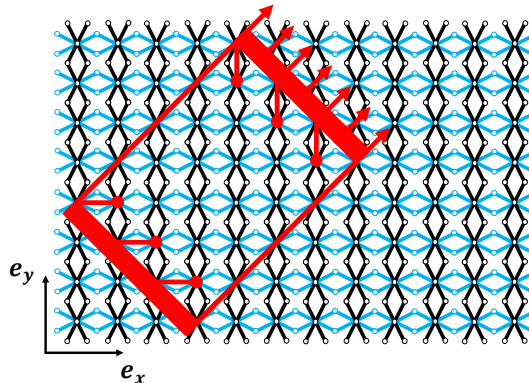


Figure 4: Bi-pantographic structure and bias extension experiment schematics.

It has been proved [1] via an asymptotic expansion homogenization that, when dealing with planar and linearized strains, bi-pantographic sheets lead to a more complete second gradient linear two-dimensional continuum. However, still not all second gradients of the placement field appear. Namely, mixed (with respect to material symmetry directions) second spatial derivatives of the placement field do not appear in the deformation energy density of such a continuum. Never-

theless, the very nature of the mechanical architected structure of bi-pantographic sheets implies that the geometric nonlinearities arise “very early” in every deformation pattern (see for a discussion of this point [19]). Therefore, the homogenization process needs to be performed for the case of large strains if one intends to compare modelling with experiments. We briefly introduce homogenization results for bi-pantographic structures in large strains and then predictions obtained using such second gradient model are compared with experimental evidence.

The specific objective of the present paper is to present a preliminary comparison between the predictions of the novel second gradient continuum, briefly introduced herein, for bi-pantographic sheets with experimental evidence obtained by DIC [12] in bias extension test performed on Polyamide 2200 SLS 3D-printed specimens.

2 Asymptotic homogenization of bi-pantographic architectures

Let us denote the reference domain of the body as Ω and let $\chi : \Omega \rightarrow \mathbb{R}^2$ be the placement function. The homogenized energy obtained heuristically for the lattice length $\varepsilon \rightarrow 0$ in the case of non-linear strains is the following

$$\begin{aligned} \mathcal{E} = & \int_{\Omega} \sum_{\alpha=x,y} \left\{ K_E K_F \left[\frac{\frac{3}{4}\rho_{\alpha}^2 - 1}{\frac{3}{4}\rho_{\alpha}^2 (K_E - 6K_F) - K_E} \left(\frac{\partial \vartheta_{\alpha}}{\partial \alpha} \right)^2 \right. \right. \\ & \left. \left. + \frac{\frac{3}{4}\rho_{\alpha}^2}{\left(1 - \frac{3}{4}\rho_{\alpha}^2\right) [8K_F + \rho_{\alpha}^2 (K_E - 6K_F)]} \left(\frac{\partial \rho_{\alpha}}{\partial \alpha} \right)^2 \right] \right. \\ & \left. + K_S \left[\cos^{-1} \left(1 - \frac{3}{2}\rho_{\alpha}^2 \right) - \pi + 2\gamma \right]^2 \right\} dA \end{aligned} \quad (1)$$

with ρ_{α} and ϑ_{α} used in order to rewrite the tangent vector field $\frac{\partial \chi}{\partial \alpha}$ to deformed material lines oriented along the axis e_{α} in the reference configuration as

$$\begin{aligned} \frac{\partial \chi}{\partial x}(x, y) &= \rho_x(x, y) \{ [\cos \vartheta_x(x, y)] e_x + [\sin \vartheta_x(x, y)] e_y \} , \\ \frac{\partial \chi}{\partial y}(x, y) &= \rho_y(x, y) \{ [\cos \vartheta_y(x, y)] e_y + [\sin \vartheta_y(x, y)] e_x \} . \end{aligned} \quad (2)$$

Thus ρ_{α} corresponds to the norm of the tangent vector $\left\| \frac{\partial \chi}{\partial \alpha} \right\|$ to the deformed material lines directed along e_{α} in the reference configuration.

3 Comparison of numerical predictions with experimental evidence

Tested specimens were 3D-printed using Selective Laser Sintering (SLS) procedure (Figs. 5 and 6). Polyamide powder was used as raw material (see Fig. 5 (A) and (C)). Hard-device conditions in Fig. 4, i.e. bias extension test, were realized 1. by ‘welding’ to the two clamping regions the adjacent elements, such clamping regions being gripped by the loading machine 2. by connecting with stocky rhomboidal elements (meant to be rigid with respect to other elements of the specimen for the considered load range) adjacent hinge axes in the vicinity of gripping areas.

Fig. 6 (B) shows the different pieces constituting the designed bi-pantographic prototype: 1. short slender elements meant to mainly bend and extend (black square), 2. cylinders meant to be mainly twisted (green square), and 3. hinges connecting short slender elements at middle points (red square). It is worth to stress out that the specimen was printed as a whole piece, without the need for additional assembly of the joints. The specimen is made by eight layers, each one hosting a family of parallel equispaced slender elements, giving for a total thickness of the specimen equal to 13.4 mm.

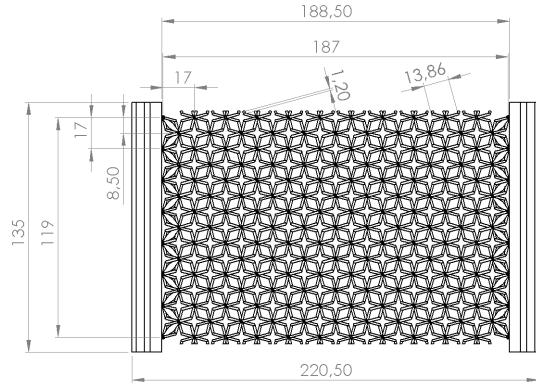


Figure 5: Technical drawing of bi-pantographic prototypes. All lengths are expressed in *mm*.

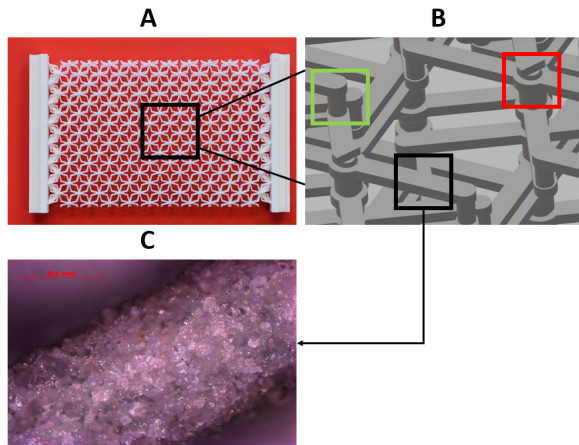


Figure 6: Full top-view of additively manufactured bipantographic fabrics especially designed for bias extension test (A). Zoomed view of microstructure realization in Computer Aided Design (B). Zoomed view of short slender elements obtained by optical microscopy (C).

Digital Image Correlation (DIC) is used to measure the displacement of two sets of points (Fig. 7 (left)). The red points correspond to the hinges interconnecting the two families of pantographic beams, while the blue points depict one series of auxiliary hinges, namely those internal to a given pantographic beam. For the sake of readability only one of the two possible sets of auxiliary hinges are shown in Fig. 7 (left). In the present case, local DIC analyses are performed, in which interrogation windows are centered about each considered hinge. The average translation is evaluated by maximizing the correlation product, which is computed via fast Fourier transform. The size of each interrogation window is equal to 50 pixels (or 6.3 mm). This length is about one third of the distance between two neighboring principal hinges in the vertical and horizontal directions (see Fig. 7 (left)). It is worth noting that the elementary cell of the homogenization model would also consider this characteristic length-scale.

Fig. 7 (right) shows the deformed shape when a displacement of 30 mm was prescribed to the sample. In the present case the analyses consisted of the registration of 60 images (i.e. 0.5 mm increment each). An incremental procedure was followed, namely displacement increments were measured by updating the picture of the reference configuration (becoming the picture of the deformed configuration of the previous increment). Such procedure allows the rigid body translation hypothesis of the matter inside the interrogation window to be a good approximation of the local kinematics. Furthermore it enables very large displacements amplitudes to be measured (in the present case the maximum displacement is equal to about 250 pixels).

The image elaboration which has been obtained

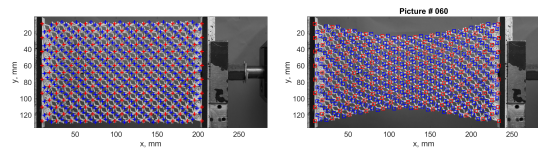


Figure 7: Local Digital Image Correlation of experimental data. Reference configuration (left) and 60th picture corresponding to a prescribed displacement equal to 30 mm (right).

shows some not standard deformation patterns. In particular the material lines constituted by the pantographic beams and “materialized” by the red squares of Fig. 7 (right) show a change of geodesic curvature, which is the kinematic signature of higher order continua equilibrium. We are not aware of first gradient continua showing such characteristic deformation for a tensile test. It is worth noting that in pantographic sheets (which are already second gradient but less complete continua) material curves having only one curvature (see, e.g., [4]) have been observed. Concerning the points labeled with blue squares it has to be remarked that they are approaching one to the other, as opposed to the red points that see their separation increase. As a consequence it is not possible to introduce a unique homogenized displacement field consistently accounting for the displacements of all red and blue points. This observation confirms the theoretical considerations presented in [7]. The fact the blue points see their distance decrease and become less than the interrogation window size may cause some registrations to be less satisfactory. Special care should be exercised for very large deformations when using the present registration procedure.

Fig. 8 shows the comparison between predicted and measured displacements of the primary hinges, for two prescribed overall displacements. This model has been described in the previous section and it is capable, by construction, to predict the displacement of the red points, only. The three material parameters of the used second gradient continuum are calibrated with a simple “best fit” procedure, which is, however, initialized by a theoretically established first conjecture identification (see [4]). The data used in the identification procedure are two shearing angles derived from experimental displacements shown in Fig. 8 and the resultant force. Albeit only three independent parameters are used in the calibrated model very good agreement is observed for the 173 hinges positions (in Fig. 8 (left)). With the same parameters set, the model is validated in Fig. 8 (right). Fig. 8 compares the experimental and predicted total reaction force versus prescribed displacement.

4 Conclusions

In this paper we have synthesized a 2D continuum whose deformation energy depends on i) the geodesic curvature of the D4 directions of material symmetry, ii) the derivatives of elongations along D4 directions with respect to these directions and iii) the first gradient shear strain. It has to be remarked that the strains defined in ii) are first introduced for bi-pantographic sheets. The constitutive parameters needed in the model formulation reduce to three only.

Some experimental evidence is gathered, in an extension test, for a 3D printed specimen via local and incremental DIC analyses. In addition to the measurement of the detailed kinematics of various hinges, the 3 material parameters K_E , K_S , K_F could be calibrated, and the model validated in large deformation modes.

It is concluded that the architected material mathematically designed in [1] allows for large elastic deformations in two independent material directions. It is expected that such a mechanical behavior may be of great interest in various applications, like in fiber-reinforced materials[33]. Future outlooks include the study of bi-pantographic structures by means of discrete and semi-discrete modelling [27, 28, 30] and the search for exotic solutions [29] enabled by strong nonlinearities.

Acknowledgment

Authors thank Tomasz Lekszycki (Warsaw University of Technology) for stimulating discussions.

References

- [1] Sepecher P, Alibert J.J., dell’Isola F. (2011). Linear elastic trusses leading to continua with exotic mechanical interactions. In J. of Physics: Conference Series vol. 319 pp. 12-18. IOP Publishing.
- [2] Alibert JJ, Sepecher P, dell’Isola F. (2003). Truss modular beams with deformation energy depending on higher displacement gradients. *Mathematics and Mechanics of Solids* 8, 51-73.
- [3] Steigmann, David J., and Francesco dell’Isola (2015). Mechanical response of fabric sheets to three-dimensional bending, twisting, and stretching. *Acta Mechanica Sinica* 31.3 : 373-382.
- [4] dell’Isola, F., Giorgio, I., Pawlikowski, M., & Rizzi, N. L. (2016). Large deformations of planar extensible beams and pantographic lattices: heuristic homogenization, experimental and numerical examples of equilibrium. *Proceedings of the Royal Society A: Mathematical, Physical and Engineering Sciences*, 472(2185).

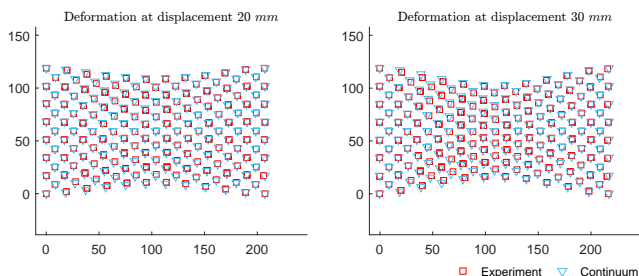


Figure 8: Comparison of points in red color in Fig. 7 (left) between continuum modelling simulation and experiments. The agreement is excellent within measurement tolerances.

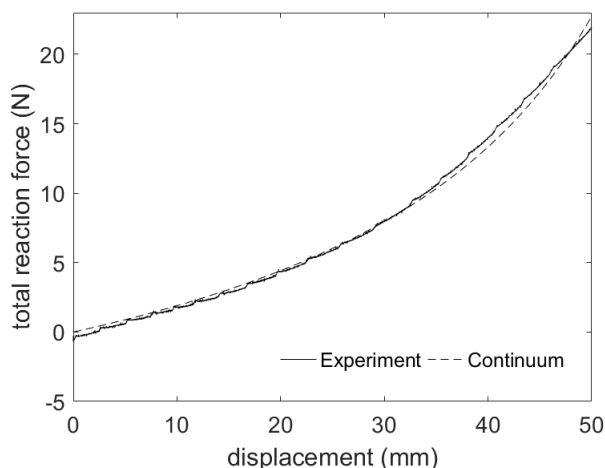


Figure 9: Total reaction force versus prescribed displacement for continuum modelling and experiment.

- [5] dell’Isola, F., Lekszycki, T., Pawlikowski, M., Grygoruk, R., & Greco, L. (2015). Designing a light fabric metamaterial being highly macroscopically tough under directional extension: first experimental evidence. *Zeitschrift für angewandte Mathematik und Physik*, 66(6), 3473-3498.
- [6] Placidi, Luca, Ugo Andreaus, and Ivan Giorgio (2017). Identification of two-dimensional pantographic structure via a linear D4 orthotropic second gradient elastic model. *Journal of Engineering Mathematics* 103.1 : 1-21.
- [7] Abdoul-Anziz, Houssam, and Pierre Seppecher (2018). Strain gradient and generalized continua obtained by homogenizing frame lattices. *Mathematics and mechanics of complex systems* 6.3 : 213-250.
- [8] Eremeyev, V.A., Alzahrani, F.S., Cazzani, A., dell’Isola, F., Hayat, T., Turco, E., Konopińska-Zmysłowska, V. On existence and uniqueness of weak solutions for linear pantographic beam lattices models (submitted). *Continuum Mechanics and Thermodynamics*. 26 pp.
- [9] Pideri, Catherine, and Pierre Seppecher (1997). A second gradient material resulting from the homogenization of an heterogeneous linear elastic medium. *Continuum Mechanics and Thermodynamics* 9.5 : 241-257.
- [10] Briane, Marc, and Mohamed Camar-Eddine (2007). Homogenization of two-dimensional elasticity problems with very stiff coefficients. *Journal de mathématiques pures et appliquées* 88.6 : 483-505.
- [11] Toupin, R. A. (1964). Theories of elasticity with couple-stress. *Archive for Rational Mechanics and Analysis*, 17(2), 85-112.
- [12] Sutton, Michael A., Jean Jose Orteu, and Hubert Schreier. *Image correlation for shape, motion and deformation measurements: basic concepts, theory and applications*. Springer Science & Business Media, 2009.
- [13] Kron, G. (1943). Equivalent circuits to represent the electromagnetic field equations. *Physical Review*, 64(3-4), 126.
- [14] Kron, G. (1945). Electric circuit models of the Schrödinger equation. *Physical Review*, 67(1-2), 39.
- [15] dell’Isola, F., Maurini, C., & Porfiri, M. (2004). Passive damping of beam vibrations through distributed electric networks and piezoelectric transducers: prototype design and experimental validation. *Smart Materials and Structures*, 13(2), 299.
- [16] Andreaus, U., dell’Isola, F., & Porfiri, M. (2004). Piezoelectric passive distributed controllers for beam flexural vibrations. *Modal Analysis*, 10(5), 625-659.
- [17] Porfiri, M., dell’Isola, F., & Frattale Mascioli, F. M. (2004). Circuit analog of a beam and its application to multimodal vibration damping, using piezoelectric transducers. *International Journal of Circuit Theory and Applications*, 32(4), 167-198.
- [18] Lossouarn, B., Deü, J. F., & Aucejo, M. (2015). Multimodal vibration damping of a beam with a periodic array of piezoelectric patches connected to a passive electrical network. *Smart Materials and Structures*, 24(11), 115037.
- [19] Eremeyev, V. A., dell’Isola, F., Boutin, C., & Steigmann, D. (2018). Linear pantographic sheets: existence and uniqueness of weak solutions. *Journal of Elasticity*, 132(2), 175-196.
- [20] Barchiesi, E., dell’Isola, F., Laudato, M., Placidi, L., & Seppecher, P. (2018). A 1D Continuum Model for Beams with Pantographic Microstructure: Asymptotic Micro-Macro Identification and Numerical Results. In *Advances in Mechanics of Microstructured Media and Structures* (pp. 43-74). Springer, Cham.
- [21] Barchiesi, E., Eugster, S.R., Placidi, L., & dell’Isola, F. Pantographic beam: A complete second gradient 1D-continuum in plane (submitted). *Zeitschrift für angewandte Mathematik und Physik*.
- [22] Boutin, C., Giorgio, I., & Placidi, L. (2017). Linear pantographic sheets: Asymptotic micro-macro models identification. *Mathematics and Mechanics of Complex Systems*, 5(2), 127-162.
- [23] Milton, G., Briane, M., & Harutyunyan, D. (2017). On the possible effective elasticity tensors of 2-dimensional and 3-dimensional printed materials. *Mathematics and Mechanics of Complex Systems*, 5(1), 41-94.
- [24] Milton, G., Harutyunyan, D., & Briane, M. (2017). Towards a complete characterization of the effective elasticity tensors of mixtures of an elastic phase and an almost rigid phase. *Mathematics and Mechanics of Complex Systems*, 5(1), 95-113.
- [25] Giorgio I., Culla A. & Del Vescovo D. (2009) Multimode vibration control using several piezoelectric transducers shunted with a multiterminal network. *Archive of Applied Mechanics*, 79, 859–879.
- [26] Turco, E., Golaszewski, M., Giorgio, I. & D’Annibale, F. (2017) Pantographic lattices with

non-orthogonal fibres: Experiments and their numerical simulations. *Composites Part B: Engineering*, 118:1–14.

- [27] Andreaus, U., Spagnuolo, M., Lekszycki, T., & Evgster, S. R. (2018). A Ritz approach for the static analysis of planar pantographic structures modeled with nonlinear Euler–Bernoulli beams. *Continuum Mechanics and Thermodynamics*, 30(5), 1103-1123.
- [28] Turco, E. (1998). Load distribution modelling for pin-jointed trusses by an inverse approach. *Computer Methods in Applied Mechanics and Engineering*, 165(1-4), 291-306.
- [29] Baroudi, D., Giorgio, I., Battista, A., Turco, E. & Igunnov L. A. (2019) Nonlinear dynamics of uniformly loaded Elastica: Experimental and numerical evidence of motion around curled stable equilibrium configurations, *ZAMM - Zeitschrift für Angewandte Mathematik und Mechanik*, 99(7): e201800121-1–20. (DOI:10.1002/zamm.201800121)
- [30] Turco, E. Tools for the numerical solution of inverse problems in structural mechanics: review and research perspectives (2017) *European Journal of Environmental and Civil Engineering*, 21 (5), pp. 509-554. DOI: 10.1080/19648189.2015.1134673
- [31] De Angelo, Michele, Mario Spagnuolo, Francesco D’annibale, Aron Pfaff, Klaus Hoschke, Aviral Misra, Corinne Dupuy, Patrice Peyre, Justin Dirrenberger, and Marek Pawlikowski. "The macroscopic behavior of pantographic sheets depends mainly on their microstructure: experimental evidence and qualitative analysis of damage in metallic specimens." *Continuum Mechanics and Thermodynamics* (2019): 1-23.
- [32] Altenbach, H., Birsan, M., and Eremeyev, V. A. (2013). Cosserat-type rods. In *Generalized Continua from the Theory to Engineering Applications* (pp. 179-248). Springer Vienna.
- [33] Avella, M., Dell’Erba, R., & Martuscelli, E. (1996). Fiber reinforced polypropylene: Influence of iPP molecular weight on morphology, crystallization, and thermal and mechanical properties. *Polymer composites*, 17(2), 288-299.